

semiconductor material. The quadratic photo-response of such devices may also occur due to SHG either in bulk LED material (GaAs) or at the asymmetric interfaces, even for centro-symmetric materials. At Laser Plasma Division of RRCAT, polarization dependence of the quadratic photocurrent in AlGaAs based LEDs and characteristics of CP-AC signals have been studied to distinguish the two processes, using a 200 fs duration laser beam from a cw mode-locked laser oscillator.

Typical induced photocurrent of the AlGaAs LED recorded w. r. to the angle of rotation of the half wave plate is depicted in Fig.L.14.1a. It is seen that the induced current changes periodically with orientation of linear polarization of the laser beam. Next, the CP-AC signals have been recorded using modified Michelson interferometer. A properly oriented quarter wave plate is kept in its one arm in order to have cross-polarized beam and a rotating half-wave plate was placed at output of interferometer to get different polarization orientations relative to a given crystal axis of LED sample. The variation of the induced quadratic current for LED with respect to the angle of rotation of the half wave plate corresponding to maximum, minimum and pedestal values of cross-polarized autocorrelation (CP-AC) signal is shown in Fig.L.14.1b. Corresponding to this variation, the CP-AC signals with maximum and minimum fringe visibility are also depicted in upper and lower traces of Fig.L.14.2.

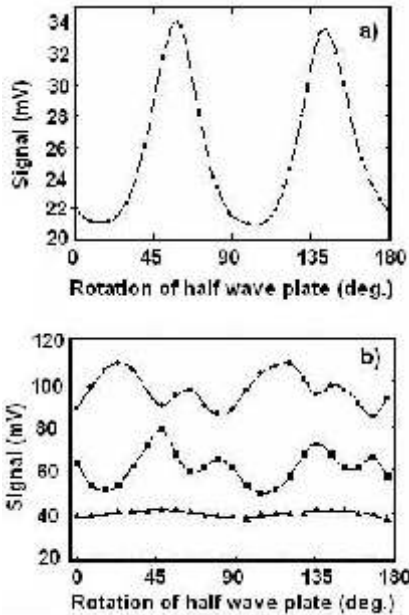


Fig.L.14.1: Typical variation of quadratic photocurrent (a: upper) and variation of maxima, minima and pedestal of CP-AC signals (b: lower) recorded using 200 fs laser pulses from cw mode-locked laser oscillator.

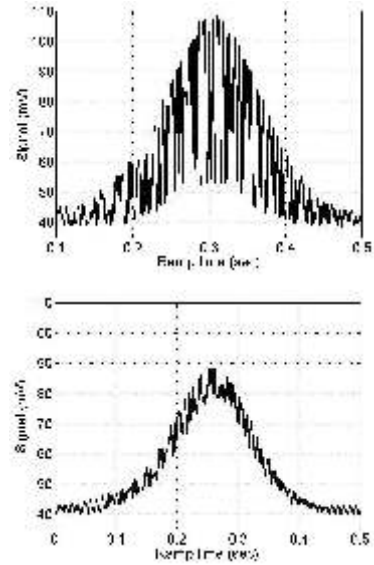


Fig.L.14.2 : Upper and lower traces depict CP-AC signals with maximum and minimum fringe visibility respectively.

A theoretical model has also been developed for CP-AC signals for given polarization relative to crystal axis of the sample. This model accounts for variation of CP-AC signals obtained in case of pure TPA or pure SHG case. By comparing the theoretical and experimentally recorded variation of CP-AC signals, one can estimate the relative contributions of third order non-linearity responsible for TPA and second order non-linearity governing SHG in a given sample, which is otherwise very difficult in case of commercial semiconductor photo devices. [For more details, see : A. K. Sharma, P. A. Naik, and P. D. Gupta, *Applied Physics B (Laser & Optics)* 88, 67, 2007]

Contributed by :

A. K. Sharma (aksharma @ cat.ernet.in) and P. A. Naik

L.15 : Long distance optical guiding of colloidal particles inside the focal region of a holographic axilens

Optical guiding uses the radial gradient force to localize a particle to the beam axis and the radiation pressure or scattering force of the beam to propel the particle along the axis of the beam. For a tightly focussed Gaussian laser beam required to ensure localization of particles on the beam axis, the guiding distance is \sim Rayleigh range and hence quite short. The use of non-diffracting Bessel beam or the extended focal depth achieved by focussing a super continuum beam, have therefore been used to extend the guiding distance. However, in both these approaches, the enhancement in the guiding distance comes at a price. For Bessel beam, the energy is distributed in several rings and therefore there is

poor utilization of available power which results in lower guiding velocity. Focussed super continuum beam is not suitable for guiding biological objects because the extended spectral range leads to concern about absorption induced damage. Laser Bio-Medical Applications and Instrumentation Division of RRCAT has shown that an aspheric holographic optical element (axilens), which combines the long depth of focus of axicons and the good light collection efficiency of a spherical lens, can lead to significant enhancement in the guiding distance without much compromise on the guiding velocity.

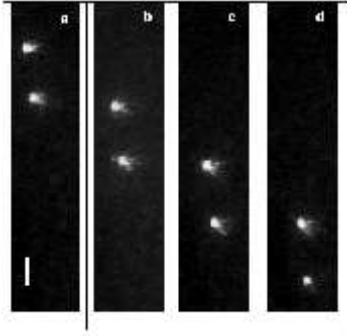


Fig.L.15.1. Guiding of two 6 μm PS microspheres inside the focal region of a holographic axilens. The laser beam direction appears as from top to bottom. The microspheres were imaged using the laser light scattered by them. With the optics used, the size of the image of the particles on the camera was $\sim 16 \mu\text{m}$. Successive frames are separated in time by 4 s. Scale bar is $45 \mu\text{m}$ long.

A holographic axilens was generated by applying an appropriate phase hologram pattern on a spatial light modulator (SLM, LCR-2500 Holoeye Photonics). The output of a 532 nm, cw laser source (Verdi, Coherent Inc) was focussed using this axilens onto a glass cuvette containing $\sim 6 \mu\text{m}$ polystyrene (PS) spheres suspended in aqueous medium. The sample was imaged using a combination of a 10X microscope objective and a CCD camera. Fig.L.15.1 shows guiding of two PS microspheres. The bright spots correspond to the laser light scattered by the microspheres. Fig.L.15.2 shows the measured variation of guiding velocities along the direction of the transport of the particles when a holographic axilens or a spherical lens of identical focal length ($\sim 200 \text{ mm}$) were used to focus the beam. The beam powers ($\sim 100 \text{ mW}$) was also kept same for this experiment. Compared to the use of a spherical lens, a factor of ~ 2.5 larger guiding distances was achieved using the axilens. Although the peak guiding velocity was $\sim 35\%$ less with axilens, the guiding velocity was more uniform over the distance of transport. The observed guiding distance ($\sim 10 \text{ mm}$) using axilens is significantly longer than that reported previously ($\sim 3 \text{ mm}$).

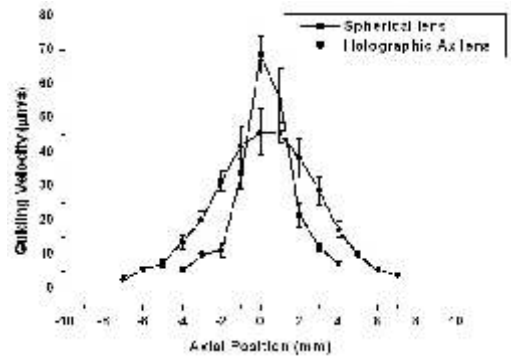


Fig.L.15.2. The guiding velocities vs axial position plot inside the focal region of a holographic axilens and a spherical lens.

*Contributed by :
S. Ahlawat, R.S. Verma, R. Dasgupta
(raktim@cat.ernet.in), and P. K. Gupta*

L.16 : Narrow band x-ray emission in the water-window spectral region

X-ray sources in the water-window region (23–44 Å) are of particular interest for imaging of live biological samples with high contrast, as in this range, the water present in the sample offers very little absorption to the radiation compared to the other major constituents like carbon. Laser produced plasmas, on account of their high peak brightness, can provide sufficient exposure in a single radiation pulse of short duration (nanosecond or smaller). This facilitates imaging of the sample in a single shot which is advantageous as it prevents any degradation to resolution due to motion blurring, as well as radiation induced structural changes in the sample which manifest over a longer time scale.

Laser irradiated gas and liquid jets have been used to produce narrow band line emission in the water-window spectral region, and they are accompanied by little or no plasma-debris. However they have rather poor conversion of laser energy to x-rays. On the other hand, the use of high-Z solid targets and short wavelength lasers as the driver for producing a laser-plasma x-ray source of high conversion efficiency is well established. More recently, novel targets have been explored such as nanostructure targets and mix-Z targets for enhancement of the x-ray emission. A debris-free x-ray radiation in the water-window spectral region can be obtained from these plasmas by using them along with either multi-layer x-ray mirror or narrow band x-ray filters. Free-standing x-ray filters will have the advantages of a simple geometry and they are available with good transmission ($\geq 10\%$) over a narrow spectral band. X-ray imaging using broadband radiation within the water-window spectral region may also lead to a poor contrast and a lower resolution in the